Surface-Binding Forms of Carboxylic Groups on Nanoparticulate TiO_2 Surface Studied by the Interface-Sensitive Transient Triplet-State Molecular Probe

Yu-Xiang Weng,* Long Li, Yin Liu, Li Wang, and Guo-Zhen Yang

Institute of Physics, Chinese Academy of Sciences, Beijing 100080, P. R. China

Received: December 6, 2002; In Final Form: February 13, 2003

Surface binding between the carboxylic group and the TiO_2 nanoparticle is important in the potentially applicable dye-sensitized mesoporous TiO_2 crystalline solar cell. However, the nature of the surface binding is still not clear enough. We propose a new method to study the surface binding between the carboxylic group and the TiO_2 surface atoms by using an interface-sensitive molecular probe. The principle underlying this method is based on the triplet−triplet absorption of the probe molecule all-*trans*-retinoic acid (ATRA) formed by the photoinduced charge recombination between the TiO_2 nanoparticle and the probe molecule. By characterizing the individual triplet absorption spectra of ATRA in different forms, including the synthesized ester-like linkage model compound tri-butoxyl titanium (IV) all-*trans*-retinoate ($Ti(IV)(OBu)_3RCOO$; RCOO = retinoate), the composition of different surface binding forms of carboxylic groups on TiO_2 nanoparticle surfaces in hexanol has been determined. The result shows that the simple adsorption form (anion, hydrogen bonding) comprises about 3% of the total adsorbed form, the ester-like form accounts for 63%, and chelating together with bridging form accounts for 34%.

Introduction

A "monomolecular layer" of redox or photoactive molecules on the semiconductor surface is an important strategy in designing molecule-based devices,[1] quantum dot devices,[2] photocatalysis,[3] and solar energy conversion.[4,5] This strategy requires that the assembled molecule have at least one anchoring group to form binding with the semiconductor surface atoms. Among various kinds of anchoring groups, the carboxylic group has proved to be an efficient interfacial linkage in the dye-sensitized wide-band-gap semiconductor TiO_2, which constitutes one of the elemental steps in the construction of a potentially applicable solar cell.[6−8] The most efficient dye for solar conversion is $Ru(dcbpy)_2(NCS)_2$ (RuN3; dcbpy = 4,4′-dicarboxy-2,2′-bipyridine).[8] For its high solar energy conversion efficiency, adsorption of ruthenium dye onto the TiO_2 surface has been intensively studied.[9,10] The ruthenium complex dye contains two bipyridine ligands with 4,4′ substitution by two carboxylic acid groups. Because of the steric effect, only two of the four carboxylic groups can be attached to the TiO_2 surface. Owing to the tight linkage between RuN3 and the TiO_2 surface via the carboxylic group, the photoinjection of electron from the excited state of the dye molecule to the conduction band of the semiconductor can be very efficient.[11−13] It has been proposed that the surface species can be in several different forms, including the simple adsorption by electrostatic attraction, hydrogen bonding, or chemical bond formation of ester-like linkage, bridging, and chelating (Scheme 1).[14]

Among various adsorption forms, chemical bonding provides a strong interfacial link between the dye molecules and the TiO_2 surface.[15,16] Attempts to correlate efficiency of the solar energy conversion to the surface binding form have been reported, which suggests that the surface binding forms play an important role in determining the solar conversion efficiency, as well as the stability of the cell.[17] Therefore, it is important to understand the compositions of the surface binding forms and the mechanism of these different forms in mediating the interfacial electron-transfer process. However, the nature of the interaction between the carboxylic group and the TiO_2 surface atoms still remains as a subject of debate.[18,19]

SCHEME 1: (a) Anion, (b) Ester-Like Linkage, (c) Chelating, (d) Bridge, (e) Single H-Bonding, (f) Double H-Bonding

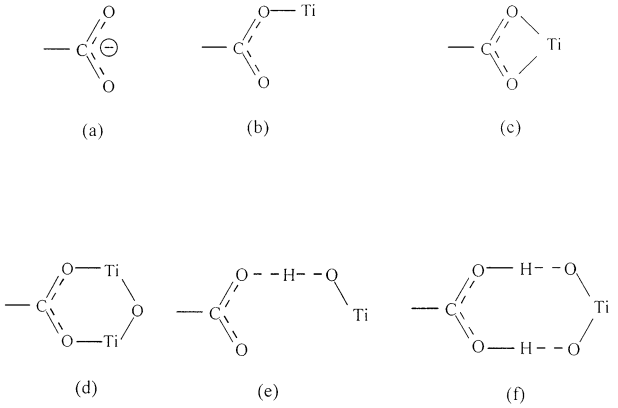

In the earlier studies, the pyridine carboxylic molecule was chemically attached to the TiO_2 surface by means of chemical reaction between the carbonyl chloride with the hydroxyl groups on the TiO_2 surface. In such a reaction, an ester-like bond is expected to be formed at the surface. Then ruthenium complex dye was synthesized directly at the interface by complexation of the ruthenium atom with the pyridine carboxylic ligand already bounded to the titanium surface atoms. Thus the linkage between the carboxylic group of the ruthenium complex dye and the TiO_2 surface was presumed to be an ester-like linkage.[20,21]

* To whom correspondence should be addressed. Tel: +86-10-82649342. Fax: +86-10-82649451. E-mail: yxweng@aphy.iphy.ac.cn.

10.1021/jp022534n CCC: $25.00
Published on Web 04/12/2003

Later, various techniques including vibrational spectroscopy,[14,18] infrared-visible sum frequency generation,[22] X-ray photoemission spectrum (XPS),[23] and the single molecule analysis by noncontact atomic force microscopy[24] have been employed to detect the surface bonding between the carboxylic group and TiO_2 surface. Among these, vibrational spectroscopies are the most informative means for the structural assignment of the surface binding. Though the experimental observation of vibrational modes for surface binding are similar among different groups,[14,15,18,25] the assignments of the surface binding forms are controversial. For the dye of multi-carboxylic anchoring groups, owing to the steric effect, not all the carboxylic groups can be attached onto the surface of the TiO_2 crystalline, leaving some of the carboxylic groups in a protonated form in an acidic medium. Therefore, the main discrepancy arises in the assignment of C═O vibrational frequency around 1700 cm^{-1} to the ester-like linkage form or to the carboxylic group.

The nature of the surface bonding between the carboxylate group and the TiO_2 surface atom was studied for the first time with resonance Raman spectroscopy by Umapathy et al,[26] and they concluded that at pH 4 ruthenium complex dyes are physisorbed through a solvation layer. Couzis et al studied dynamically the interfacial interaction between the alumina surface and the carboxylic group by use of attenuated total reflection Fourier transform infrared spectroscopy (ATR-FTIR) which is a sensitive method for the interface detection.[27,28] They concluded that the laurate (carboxylate-bearing molecule) ion can react with the alumina through a water abstraction reaction forming a unidentate aluminum salt, and different surface species are formed at varied pH values. Meyer et al studied the resonance Raman spectra of ruthenium (II) bipyridine [2,2′-bipyridyl]-4,4′-dicarboxylate ([$Ru(bpy)_2$(bpdc)]) on the surface of powered TiO_2; a 1691 cm^{-1} Raman mode which can be attributed to the vibrational mode of ester-like linkage was observed, and they suggested that the surface attachment is via an ester-like linkage or via hydrogen bonding.[14] They also proposed a possible mechanism for the formation of the surface ester bond by a water abstraction reaction between TiO_2 surface hydroxyl group and the carboxylic group. Murakoshi et al studied the IR reflectance spectra of RuN3 adsorbed to Degussa P25 and to nanocrystalline TiO_2;[15] they observed an IR vibrational mode at 1732 cm^{-1}, and concluded that both ester linkage and chelation occur. They also showed that a reflux treatment of the dye/TiO_2 system in ethanol solution promoted ester binding and enhanced the photon-to-electron conversion efficiency. Duffy et al also studied the internal reflection IR spectroscopy of RuN3 adsorbed on TiO_2 sol−gel film at different PH.[25] At pH 2, an absorption band at about 1720 cm^{-1} was observed, and at pH 6.3, this band disappeared. They assigned this band to the free carboxylic acid. In a recent paper, Fennie et al studied the IR and Raman spectra of RuN3 attached onto the TiO_2 film;[18] they found that the intensity of absorption band around 1740 cm^{-1} dropped significantly when the TiO_2 film was treated with weak base. In addition, they analyzed the frequency difference between the asymmetric and symmetric vibration of COO^-, and concluded that the 1740 cm^{-1} can be arising from the free carboxylic acid, and bidentate chelating or bridging is the major link between the TiO_2 surface and the dye. Other works supporting either the ester-like linkage or the bridge as the major form can be found.[29,30]

Because the formation of ester-like linkage form is believed to be dependent on the pH value of the system, and RuN3 has a free carboxylic group when it attaches onto the TiO_2 surface, these factors render an uncertainty in the assignment when using 1700 cm^{-1} as an indication of ester bond formation. Therefore, new detection methods are necessary to reexamine the surface binding forms of carboxylic group on TiO_2 surface.

SCHEME 2: Molecular Structure of (a) All-*trans*-Retinoic Acid and (b) 8-apo-8′-Carotenal

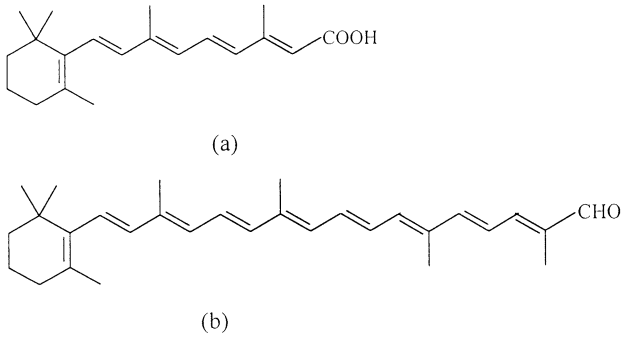

A molecular probe capable of reporting its different environments has been widely employed in studying the interfacial process. It has been successful in the study of onset of the crystallization,[31] the surface acidic sites of the zeolites,[32] micropolarity in the reverse micelles,[33] and mass transfer at a solid−liquid interface.[34] Generally, this approach is to use the molecular spectral properties such as fluorescence,[31] NMR,[32] UV−visible absorption,[33] time-resolved transient absorption,[34] etc, to report its local environment, and is specific to each case studied. In our previous work, it has been found that when all-*trans*-retinoic acid (ATRA, Scheme 2) is used to sensitize a TiO_2 colloid,[35,36] the photoinduced charge recombination between the injected electron and the oxidized dye cation follows a main channel of recombination to the triplet state which can be detected in a microsecond temporal range. Formation of the corresponding triplet state is an interfacial process. In this paper, we use ATRA as a probe molecule, which can report its binding forms on the TiO_2 surface such as free acid, deprotonated form, ester-like linkage, and probably bridging and chelating forms by its distinct triplet−triplet absorption spectra.

Experimentals

Materials. All-*trans*-retinoic acid (ATRA, Aldrich), Ti(IV) *n*-butoxide (99%) (ACROS), and 8-apo-8′carotenal (Aldrich) were used as received. Solvents and other reagents were analytical grade and used without further purification.

(a) Preparation of Tri-butoxyl Titanium (IV) all-trans-Retinoate (Ti(IV)(OBu)$_3$RCOO, RCOO = retinoate) (**1**)**.** A model compound of ester-like linkage between the carboxylic group and the Ti(IV) surface atom, i.e., tri-butoxyl titanium (IV) all-*trans*-retinoate, was prepared by the substitution of one butoxyl group with a retinoate in dichloromethane at room temperature. ATRA (6 mg) was dissolved in 15 mL of dichloromethane, then a mixture of 6.28 mg of titanium (IV) *n*-butoxide in 155 mL of dichloromethane was added. The mixed solution was kept in the dark and stirred for 1 h at room temperature. After the evaporation of the solvent, a yellow powdered mixture was obtained. The molecular weight was characterized by matrix-assisted laser desorption time-of-flight (MALDI-TOF) mass spectrometry by dissolving the yellow powder into chloroform. Besides the molecular ion peak of ATRA, the double protonated molecular ion ([$Ti(III)(OBu)_3$-$RCOO]H_2^+$) peak of the reduced form of the model compound (**1**) was observed as the parent ion peak: M/Z calculated, 568.35; found, 568.40. The isotropic distribution pattern of the protonated molecular ion is shown in Figure 1.

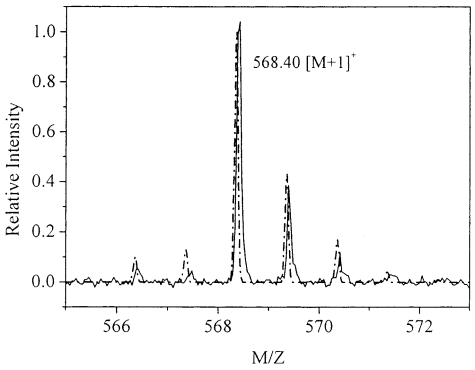

Figure 1. Isotopic distribution pattern of the double protonated molecular ion ($[Ti(III)(OBu)_3RCOO]H_2^+$, M + 1: mass of $[Ti(III)(OBu)_3RCOO]H$ plus that of a proton) of the reduced model compound (**1**). Solid line, experimentally observed pattern; dotted line, calculated pattern.

(b) Preparation of TiO_2 Colloid in Hexanol. The colloidal solution was prepared by hydrolysis of Ti(IV) *n*-butoxide in a hexanol/H_2O mixture at room temperature. Ti(IV) *n*-butoxide (0.08 g) was added into 10 mL of hexanol, and stirred for complete mixing under a N_2 gas stream. An aliquot of 1 mL of H_2O with pH preadjusted to 3.0 was added to 30 mL of hexanol, and sonicated for complete mixing. The H_2O/hexanol mixture was cooled in an ice/water bath and kept stirring, then Ti(IV) *n*-butoxide dissolved in hexanol was added dropwise under N_2 gas stream; after the completion of the reaction a clear colloidal solution was obtained. The average size of the TiO_2 particles was estimated by scanning electron micrograph (SEM) to be about 8−15 nm.

(c) Dye-Sensitization of TiO_2 Colloidal Solution. The ATRA/TiO_2 colloidal alcoholic solution was prepared by addition of concentrated ATRA methanol solution ($c = 2 \times 10^{-3}$ M) into TiO_2 colloidal solution and stirred for 30 min in the dark under a N_2 stream for dye-sensitization, keeping the apparent ATRA concentration in the bulk at 2×10^{-5} M. The resulting solution was bubbled with high purity N_2 for at least half an hour to remove the dissolved oxygen.

Measurements. The flash photolysis setup has been reported elsewhere.[35,36] Briefly, it employed the 355-nm third harmonic generation of Nd^{3+}:YAG laser as the excitation source (Quanta Ray DCR) with a pulse width (full-width-at-half-measure, fwhm) of 8 ns. When the excitation wavelength was changed to the visible region, a dye laser (Quanta Ray pulsed dye laser) was used. The probe beam source was a 500-W cw Xe lamp. The transient signal was detected by a six-stage R456 (Hamamatsu) photomultiplier tube, amplified by a 300-MHz DC amplifier (Stanford Research Systems Inc.), and finally fed into a 500-MHz digital oscilloscope (Tektronix) interfaced to a PC by a GPIB board for data handling and processing. During the experiment, the dye-sensitized TiO_2 colloidal solution was kept bubbling with an Ar gas stream.

Results and Discussion

A. Triplet-Absorption Spectra of ATRA in Different Forms. Direct excitation of ATRA by using 355-nm pulsed laser in different solvents such as CH_2Cl_2, hexane, methanol, and ethanol failed to generate any observable triplet absorption signal at the sub-microsecond temporal range, indicating a low quantum efficiency for the singlet to triplet intersystem crossing of the ATRA molecule. To increase the amount of excited-triplet-state molecules, a triplet-state sensitizer (anthrancene) was employed to increase the population of the ATRA triplet state

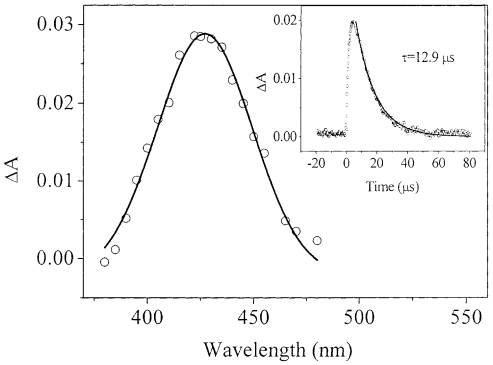

Figure 2. Triplet absorption spectrum of ATRA (2.0×10^{-5} M) in nonploar solvent hexane in the presence of anthrancene (2.0×10^{-5} M), excitation at 355 nm, 0.8 mJ/pulse. Graphic inset: the corresponding transient absorption kinetics measured at 440 nm.

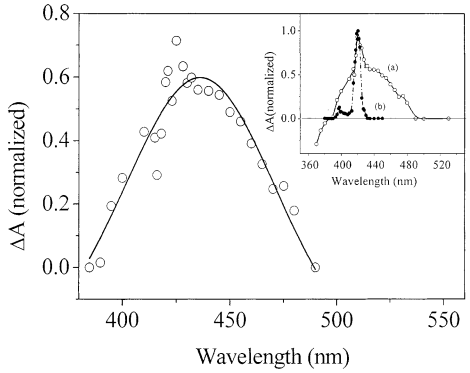

Figure 3. Spectrally resolved triplet absorption spectrum of ATRA (2×10^{-5} M) in hexanol acquired in the presence of triplet energy sensitizer anthrancene (2×10^{-5} M) excited at 355 nm, 0.63 mJ/pulse, delayed at 10 μs. Graphic inset: (a) mixed transient absorption spectra of ATRA/anthracene in hexanol (open circles), and (b) the triplet absorption spectrum of anthrancene (2×10^{-5} M) in hexanol (solid circle) excited at 355 nm, 1.0 mJ/pulse.

by intermolecular triplet-state energy transfer. To exclude interference from the triplet absorption of anthrancene itself, the triplet absorption of anthrancene in hexanol was acquired, which contains two sharp absorption peaks at 421 and 398 nm (see the graphic inset (b) in Figure 3). These two transient absorption peaks are consistent with the literature values of triplet absorption of anthrancene in different solvents, e.g., 420.3 and 398 nm in hexane,[37] and 422 and 399 nm in ethanol,[38] which were assigned to be derived from the $T_1 \rightarrow T_3$ transition.[39]

(1) Triplet Absorption Spectrum of Free ATRA in the Nonpolar Solvent. Figure 2 is the transient absorption spectrum of ATRA in the presence of anthrancene in hexane. Obviously, the spectrum is free from the contamination of the anthrancene triplet absorption, indicating an efficient triplet energy transfer from anthrancene to ATRA molecule. The transient absorption spectrum has a maximum absorbance at 427 nm, and can be fitted by a single Gaussian peak with a central wavelength at 426.9 ± 0.5 nm and a fwhm of 45.0 ± 2.6 nm. The decay kinetics can be fitted by a monoexponential decay with a time constant of 12.9 μs shown in the graphic insert. The observed triplet−triplet absorption maximum is close to the literature value of 430 nm in hexane (evaluated from the graph),[40] and that of 435 ± 5 nm in acetone.[41]

(2) Triplet Absorption Spectrum of Free ATRA in the Polar Solvent. When the medium was changed from the nonpolar solvent hexane to the polar solvent hexanol, substantial change was observed in the time-resolved transient absorbance difference spectra given in the graphic inset (a) of Figure 3, which

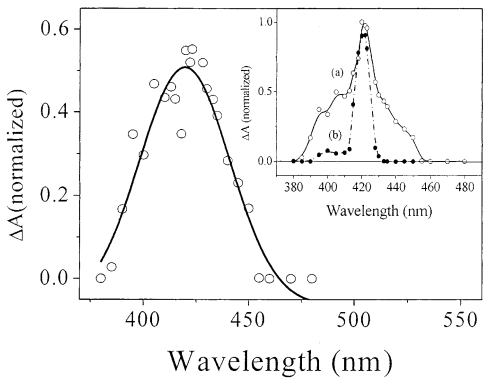

Figure 4. Spectrally resolved triplet absorption spectrum of ATRA (2×10^{-5} M) anion acquired in the presence of triplet energy sensitizer anthrancene (2×10^{-5} M) and excess *n*-butylamine (2×10^{-2} M), excited at 355 nm, 1 mJ/pulse, delayed at 10 μs. Graphic inset: (a) mixed transient absorption spectra of ATRA anion/anthracene in hexanol with excess of *n*-butylamine (open circles), and (b) triplet absorption spectrum of anthrancene (2×10^{-5} M) in hexanol (solid circle) excited at 355 nm, 1.0 mJ/pulse.

shows two sets of spectra with different kinetic feature overlap within the detected spectral region; i.e., a sharp absorption peak at 422 nm riding on the envelope of the broader one. The kinetics show that the sharp absorption peak has a fast rising, and a decay phase with a time constant of 39.5 μs, whereas the broad spectral component has a slow rise with an estimated monoexponential rise time constant about 5.4 μs, and a decay phase with a time constant of 72.2 μs. Compared to the transient triplet absorption spectrum of anthrancence (solid circle in the graphic inset (b) of Figure 3), the sharp absorption peak at 422 nm is clearly from the triplet state of anthrancene, and the remaining broad-band spectrum is assigned to the triplet absorption of ATRA formed by intermolecular triplet energy transfer. The slow rising of the ATRA triplet absorption indicates a less efficient energy transfer from the triplet state of anthrancene to that of ATRA molecule in the polar and viscous solvent hexanol with respect to that in the nonpolar solvent hexane. Therefore, the triplet absorption spectrum of ATRA in hexanol can be resolved by subtraction of an appropriately weighted anthracene T−T absorption spectrum from the total triplet absorption spectra of ATRA and anthrancene as shown in Figure 3. The line shape of the corresponding resolved spectrum can be fitted by a single Gaussian peak with a central wavelength of 436 nm and a fwhm of 69 nm. This absorption peak is also in agreement with the reported value of 440 nm in the polar medium methanol.[40] Compared to that in the nonpolar solvent hexane, the triplet absorption spectrum in the polar solvent is red-shifted and broadened.

(3) Triplet Absorption Spectrum of Free ATRA Anion in the Polar Solution. To obtain ATRA anion, excess base *tetra*-butylamine was added to the ATRA solution in the hexanol, where the concentration of *tetra*-butylamine is in large excess of that of the ATRA to guarantee the full deprotonation of ATRA. Similar to what was observed in the ATRA/anthrancene in hexanol, the transient absorption spectrum also consists of two kinds of spectra with different kinetic features shown in the graphic inset (a) of Figure 4. The sharp peak at 421 nm has a fast rising and a monoexponential decay phase with a time constant of 58.7 μs. The remaining broad band absorption has a slow rising phase with an estimated rising time constant of 5.4 μs and a monoexponential decay phase with a time constant of 62.6 μs. Accordingly, these two kinds of transient absorptions can be assigned to the simultaneous presence of triplet absorption of anthrancene and that of the ATRA anion. Figure 4 displays the corresponding transient absorption spectrum of the triplet ATRA anion obtained by removal of the contribution from the triplet absorption of anthrancene. Fitting of the triplet absorption line shape with a single Gaussian peak gives a central absorption wavelength of 420 and a fwhm of 49 nm. The fitting parameters for the T−T absorption spectrum of ATRA in hexane and hexanol, and that of ATRA anion in hexanol are listed in Table 1.

TABLE 1: Gaussian Type Fitting Parameters for the Triplet Absorption Spectra of ATRA in Different Media

solvent	λ_{max} (nm)	fwhm (nm)
hexane	426.9 ± 0.5	45.0 ± 2.6
hexanol	436.0 ± 1.23	68.8 ± 17.6
hexanol/*n*-butylamine	419.8 ± 1.7	48.9 ± 8.7

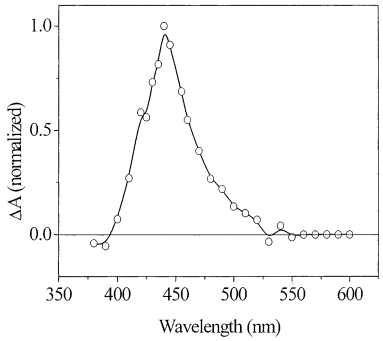

Figure 5. Transient absorbance difference spectrum of the model compound tri-butoxyl titanium (IV) all-*trans*-retinoate in CH_2Cl_2 solution containing 2×10^{-4} M ATRA and 6.0×10^{-3} M titanium (IV) *n*-butoxide, delayed at 10 μs, excited at 355 nm, 1.0 mJ/pulse.

(4) Triplet Absorption Spectrum of the Ester-Like Linkage Model Compound Tri-butoxyl Titanium (IV) all-trans-Retinoate. Because of the extreme susceptibility of the model compound to water hydrolysis, isolation of the compound (**1**) from the reaction mixture has not been successful. UV−visible absorption spectrum of the ATRA and $Ti(O-Bu)_4$ reaction mixture showed that no new absorption peak had developed other than that of ATRA. The overlap of the absorption maximum at 365 nm with that of the free ATRA in CH_2Cl_2 indicates that the UV−visible absorption spectra of both ATRA and compound (**1**) are similar in CH_2Cl_2. This will be further confirmed in a later section by the calculation based on an empirical relation between the triple−triplet transition energy and that of the singlet−singlet transition, which reveals that the expected UV−visible absorption maximum of the model compound (**1**) is at 360 nm. The transient absorption spectrum of the model compound (**1**) in CH_2Cl_2 excited at 355 nm is shown in Figure 5 which has an absorption peak at 440 nm. The transient absorption decay kinetics can be fitted by a monoexponential decay with a time constant of 36.7 μs. The transient absorption signal can be quenched by both oxygen and 8-apo-8′-carotenal, known quenchers for the triplet state.[42] A control experiment of the compound $Ti(O-Bu)_4$ and ATRA alone in CH_2Cl_2 gave no transient signal under the same condition. In addition, the free ATRA triplet absorption maximum in acetone was reported to be 435 ± 5 nm,[41] thus this absorption peak is assigned as the triplet absorption of the model compound.

B. Surface Binding of ATRA/TiO2 in Hexanol Solution. When ATRA was added to the TiO_2 colloid ethanolic solution, a new absorption band at 396 nm developed in respect to the free dye absorption at 343 nm in ethanol.[36] Whereas in the TiO_2 hexanolic solution, a new absorption band develops at 373 nm in respect to the free dye absorption at 354 nm in hexanol. When

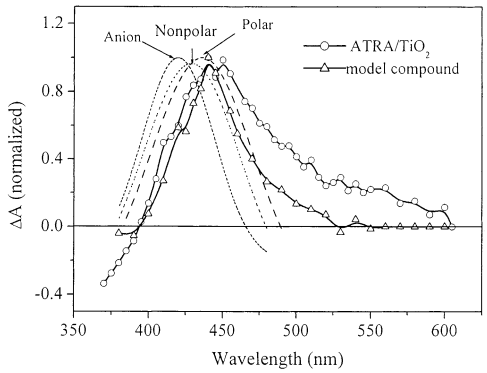

Figure 6. Transient absorbance difference spectrum of ATRA (2×10^{-5} M)/TiO_2 (2 g/L) in hexanol (open circle) delayed at 10 μs, excited at 355 nm, 0.5 mJ/pulse. Triplet absorption spectra of ATRA in hexane and hexanol, and anion in hexanol, are also presented in their Gaussian type fitting curves. The triplet absorption spectrum of the model compound is indicated by open triangle.

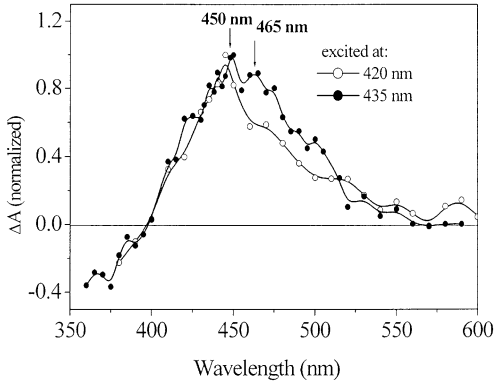

Figure 7. Normalized transient absorbance difference spectra of ATRA (2×10^{-5} M)/TiO_2 (2 g/L) in hexanol excited at two different wavelengths 420 nm, 0.50 mJ/pulse; and 435 nm, 0.45 mJ/pulse, respectively.

ATRA is excited, an electron injection from the excited state of ATRA to the conduction band of TiO_2 is expected. Figure 6 shows the transient absorbance difference spectrum of ATRA/TiO_2 in hexanol excited at 355 nm (open circle); the kinetic trace of the transient absorption signal can be fitted by a monoexponential decay with a time constant of 49.1 μs at 440 nm. The transient absorption signal around 440 nm is susceptible to oxygen quenching, but the signal around 570 nm is not sensitive to oxygen quenching. For convenience the triplet absorption spectra of different forms of ATRA (Gaussian fitted curves) and that of the model compound (**1**) (open triangle) were also presented in Figure 6 for comparison. When tuning the excitation wavelength from the UV light to the visible region, the corresponding transient absorption spectra show a systematic shift to the red region as revealed in Figure 7.

In our previous work, it has been shown, in the microsecond temporal range, that in the ATRA/TiO_2 ethanolic solution the photoinduced charge recombination between the oxidized adsorbate cation and the injected electron is mainly through the excited-triplet state rather than directly to the ground state.[36] It is noted in a very recent publication that photoinduced charge recombination between a carotenoic acid and TiO_2 colloidal nanoparticle has been observed by time-resolved absorbance difference spectroscopy within a time domain from subpicosecond to microsecond.[43] This mechanism has also been confirmed recently in our laboratory in a subpicosecond time domain by time-resolved transient absorbance difference spectroscopy. The triplet absorption spectrum acquired by a CCD in the picosecond time range is consistent with what can be observed in Figure 6.[44] The point-to-point acquired transient absorption spectrum of ATRA/TiO_2 in Figure 6 was also confirmed by sub-microsecond flash photolysis excited at 355 nm acquired by an optical multichannel analyzer (OMA) in another laboratory later. This unusual feature has been attributed to the free energy difference for the two different charge recombination channels. The interfacial charge recombination occurs mainly between the trapped electron and the oxidized ATRA cation on the TiO_2 surface. The free energy difference is estimated from the energy difference between the conduction band edge and the reduction potential of the acceptors. The charge recombination to the ground state has a driving force of $\Delta G \approx -1.2$ eV, which indicates that the back electron transfer to the ground state would lie most probably in the Marcus inverted region with a slow recombination rate.[45] On the other hand, the activation energy barrier for the charge recombination to the excited-triplet state is comparatively small owing to the small energy difference between the conduction band edge and the reduction potential of the excited-triplet state (0.3 eV).[36] This leads to a conclusion that the charge recombination through the excited-triplet state is kinetically more favorable.[43] Accordingly, the transient absorbance difference spectra observed within the micro-second time domain mainly originate from the excited-triplet state of different ATRA surface species and the corresponding radical cations. It has been reported that the absorption maximum of ATRA radical cation lies in a spectral region from 570 to 590 nm varying with the polarity of the solvents, and such an absorption signal is insensitive to the oxygen quenching.[41] Thus, the observed transient absorption within 550 to 600 nm in Figure 6 can be assigned to the ATRA radical cation absorption. The remaining blue-side absorptions, i.e., two shoulders on the absorption spectra at 418 and 435 nm, and two absorption maxima at 440 and 450 nm, together with a broad featureless absorption from 450 to 550 nm are from the excited-triplet-state absorptions of the different ATRA surface species formed by back electron transfer.

Comparing the blue-side transient absorbance difference spectrum of ATRA/TiO_2 in hexanol with those of the triplet absorption spectra of ATRA in different forms, it is obvious that the surface species of ATRA at TiO_2 consist of the following species: simple adsorbed forms containing deprotonated ATRA anion (peak at 418 nm), and ATRA in nonpolar environment (peak at 430 nm). However the relative amount of ATRA component in polar medium expected at 436 nm is negligibly small. It is interesting to note, though hexanol is a polar solvent, the triplet absorption of ATRA/TiO_2 reports its micro-environment to be of a nonpolar medium rather than a polar one. This can be understood by the nonrandom distribution of ATRA on the TiO_2 surface. Inferring from Scheme 1(e) and (f), the protonated ATRA molecules are majorly adsorbed onto the TiO_2 surface through hydrogen bonding; the carboxylic group points inward toward the TiO_2 surface while the polyene chromorphore moiety points outward toward the solvent medium. Because the polyene moiety of ATRA is hydrophobic, it is natural that the hydrophobic part of the solvent molecules would orientate toward that of the ATRA adsorbates. Therefore, a hydrophobic inner shell of micro-environment is developed around the probe molecule which in turn reports a nonploar like micro-environment.

Compared to the triplet-absorption spectrum of the model compound (**1**), it can be concluded that the predominant species absorbing at 440 nm comes from the ester-like linkage adsorbate, which is evident by the supposition of the triplet absorption

spectra of the model compound on the 440-nm absorption peak derived in ATRA/TiO_2 colloidal solution. The bridging and chelating forms have a stronger interaction with the *d* orbital of titanium atom through chemical bonding,[20] which is expected to result in a red shift in the UV−visible absorption spectra with respect to that of the ester-like linkage form. According to the linear empirical relation between the triplet−triplet transition energy and that of singlet−singlet transition for ployenes,[46] the triplet absorption of bridging and chelating forms should be red-shifted in respect to that of the ester-like linkage form. Therefore, the remaining absorption within 450 to 550 nm is attributed to the chelating and bridging forms. It is interesting to note that when the solvent changes from ethanol to the less polar solvent hexanol, the ground-state absorption of free ATRA changes from 343 to 354 nm, while the triplet absorption maximum of surface species remains unaffected; this also supports the conclusion that the surface binding species report their micro-enviroment rather than the bulk polarity.

When the excitation wavelength was tuned from 355 nm to 420 and 435 nm, the triplet absorption maxima shift from 440 and 450 to 450 and 465 nm, respectively, as shown in Figure 7, which further reveals that variation of the excitation wavelength only changes the relative intensity of the triplet absorption maxima at 450 and 465 nm. This suggests that the triplet absorption at 450 and 465 nm can arise from two different binding forms in addition to the ester-like linkage absorbing at 440 nm. Because the chelating and the bridging forms are expected to have a red-shifted UV−visible absorption spectrum when excited at the red side of the absorption spectra, more chelating and bridging forms would be excited, leading to the observed red-shift of the total triplet-absorption spectra. Thus, we tentatively assign that the 450 nm absorption is from the bridging form, whereas the absorption at 465 nm is from the chelating form. Though a "clean" ground-state absorption spectra cannot be obtained for the surface species, owing to the difficulties in obtaining the pure compounds, their ground-state absorption maxima can be evaluated by an empirical linear relationship between the singlet−singlet transition energy (ΔE_S) and the corresponding triplet−triplet transition energies (ΔE_T).[46] For a series of conjugated polyenes including retinal, carotenal, etc., the linear relation can be written as $\Delta E_T = k\Delta E_S + k^1$, where $k = 0.6$ and $k^1 = 72$ kJ/mol. We apply this relation to ATRA of known singlet−singlet and triplet−triplet transition energy for examination of the validity of this relation when the system changes from the polyene to ATRA. In hexanol, free ATRA has a triplet−triplet absorption at 436 nm, and the singlet−singlet absorption maximum evaluated from the above relation is 356 nm, very close to the measured value of 354 nm. Therefore, this empirical relation can be applied to the ATRA derivatives. By this method we have estimated the singlet−singlet absorption maximum of three different surface binding forms, and the results are listed in Table 2. In our previous work, we have applied a method to derive the triplet energy level for the ATRA, which can be summarized as $E_T = (\Delta E_S - 0.51)/2$ (eV).[36] The triplet-state energy levels of different surface species estimated by this method are also listed in Table 2. It should be noted that the evaluated singlet−singlet absorption maximum of the model compound is 360 nm, which is consistent with the UV−visible absorption spectrum of the reaction mixture of ATRA with $Ti(OBu)_4$ in CH_2Cl_2. Considering the ground-state absorption of the ester-like linkage form is almost the same as that of ATRA, the difference absorption spectrum between the ATRA adsorbates and that of free ATRA are mainly arising from the bridging and chelating forms.

TABLE 2: Photophysical Properties of Three Different ATRA/TiO_2 Surface Binding Forms in Hexanol Obtained at Different Excitation Wavelengths and that of ATRA for Comparison

exitation wavelength	λ_{max} (nm) (T−T)	λ_{max} (nm) (S_0−S_2)[a] calcd	experiment	E_T (eV)	assignment
355	440	360	365[b] (CH_2Cl_2)	1.47	ester-like
420	450	371	372 (hexanol)	1.41	bridging
435	465	388	396 (ethanol)	1.34	chelating
355	436	356	354	1.50	(ATRA/hexanol)

[a] Optical transition of S_0 to S_1 is not allowed, the lowest allowed transition is S_0 to S_2 . [b] Mixture of ATRA and the model compound.

Comparing the evaluated ground-state absorption maxima and those of experimentally observed values for the surface species, we assign that the surface species absorbing at 372 nm in ATRA/TiO_2 hexanolic solution to the ground-state absorption of the bridging form, while 396 nm in ATRA/TiO_2 ethanolic is assigned to the ground-state absorption of the chelating form. It is interesting to note that the relative ratio between bridging and chelating form seems to depend on the solvent in which the TiO_2 nanoparticle is prepared. Furthermore we have also observed that ATRA is more readily decomposed on the TiO_2 surface in ethanol than in hexanol when subjected to UV-light photolysis. This may reflect the different surface properties of TiO_2 such as oxygen deficient defect in affecting the reactivity of the surface binding form.[47,48]

C. Selective Quenching of the Surface Species with 8-apo-8′-Carotenal. As shown in Table 2, the triplet energy level for the three surface chemical binding species has the following order: ester-like linkage > bridging> chelating form. If we can choose a proper triplet energy quencher, selective quenching of the triplet states might be used to differentiate the different surface binding forms. The reported triplet energy level for 8-apo-8′-carotenal is 1.27 eV above the ground state, which is close to that of the chelating form.[46] When 8-apo-8′-carotenal was used as a triplet energy quencher, we found that the triplet absorption signal of surface species can be selectively quenched with varied efficiency, i.e., the triplet state of the chelating and bridging form is more vulnerable to the carotenal quenching. Figure 8 displays the time-resolved transient absorbance difference spectra of ATRA/TiO_2 in ethanol delayed at 10 μs at varied concentrations of the quencher. The graphic inset shows the normalized transient absorption spectrum of ATRA/TiO_2 in hexanol in the presence of 8-apo-8′-carotenal, and the triplet state absorption spectrum of the model compound is also presented for comparison, which shows that at a high concentration of the quencher almost only the ester-like linkage form can be observed. It has been reported that 8-apo-8′-carotenal has a triplet absorption maximum at 518 nm and a lifetime of 10 μs.[46,49] To avoid the spectral overlap between the triplet absorption of ATRA surface species and that of the quencher, the concentration of the quencher should be controlled below 2×10^{-4} M.[49] In the present case, the concentration of 8-apo-8′-carotenal is 2×10^{-5} M, and the interference from the spectral overlap is negligible, as was confirmed in Figure 8. Obviously the ATRA surface species serve as an energy donor, while 8-apo-8′-carotenal acts as an energy acceptor. The quenching efficiency and the triplet energy difference between the donor and the acceptor can be rationalized qualitatively by the energy gap law which has been well studied in the intramolecular energy transfer process such as internal conver-

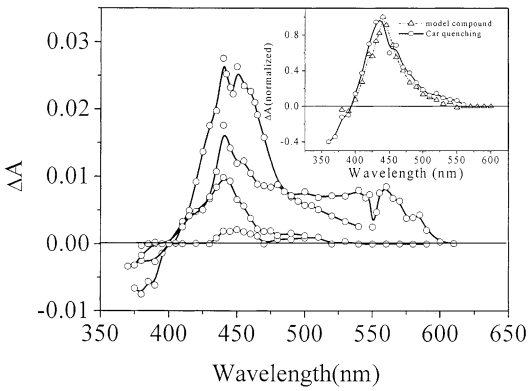

Figure 8. 8-apo-8′Carotenal quenched transient absorbance difference spectra of ATRA (2×10^{-5} M)/TiO_2 (2 g/L) in ethanolic solution at different concentrations of the quencher delayed at 10 μs. Excited at 355 nm, 1.2 mJ/pulse. The transient absorbance intensity decreases with increased concentration of the quencher in an order of $c = 0$, 1.4×10^{-5}, 2.0×10^{-5}, 4.0×10^{-5}M, respectively. Graphic inset: 8-apo-8′-carotenal (2×10^{-5} M) quenched time-resolved absorbance difference spectrum of ATRA (2×10^{-5} M)/TiO_2 (2 g/L) in hexanol (open circle), delayed at 10 μs, excited at 355 nm, 1.7 mJ/pulse; and the triplet absorption spectrum of the model compound (open triangle) for comparison.

sion.[50] However, for intermolecular triplet−triplet energy transfer for ployenes with a series of donors varying at triplet energy level, the observed tendency of quenching efficiency is opposite to what is expected from the energy gap law.[46] Our observation suggests that the triplet energy transfer occurring at the interface is more like an internal conversion process; this may reflect the unique properties of interfacially bounded molecules, and such a discrepancy remains for further investigation.

D. Compositions of the Surface Species. With the known triplet absorption spectra of several components, it is possible to make a quantitative estimation of the composition of different ATRA/TiO_2 surface species; assuming that the integrated area of the triplet absorption spectrum can quantitatively represent the different ATRA/TiO_2 surface binding forms. Accordingly, the composition of the different surface species can be estimated by the relative integrated areas of the corresponding normalized triplet−triplet absorption spectra.

The band gap of the TiO_2 semiconductor is 3.2 eV, corresponding to an absorption edge at 387 nm.[4] Therefore, 355-nm excitation could invoke direct band gap excitation creating charge carriers within the nanoparticles. An immediate effect visualized is that the injected electron and the oxidized dye radical cation would undergo recombination with their counterpart from the charge carriers, in competition with the direct charge recombination between themselves. And it is expected that the charge recombination kinetics for the trapped electron and the radical cation would be affected by the presence of the charge carrier generated by the direct band gap excitation. In the experiment, low excitation power is essential to minimizing the generation of the charge carriers. To avoid thoroughly such an effect, excitation away from the band gap excitation is imperative. Thus, two additional excitation wavelengths of 420 and 435 nm were selected. All the observed kinetics obtained at three different excitation wavelengths can be fitted by a monoexponential decay. Time constants for kinetics at some selected wavelengths excited at three different wavelengths are listed in Table 3. Comparing the kinetics of different excitation wavelength, it can be concluded that the effect of direct band gap excitation on the observed transient absorption signal at the controlled excitation power of 0.5 mJ/pulse (355 nm) is small. As shown in Figures 6 and 7, the relative compositions of various surface species depend on the excitation wavelength, therefore the compositions at different excitation wavelength are evaluated individually. For 355 nm excitation, the surface species are divided into three components: i.e., simple adsorbates including ATRA (hydrogen bonded and non-hydrogen bonded) plus its anion, the ester-like linkage form, and the bridging plus chelating forms. In the selective quenching experiment, the transient absorption spectra of ATRA/TiO_2 in hexanol in the presence of 8-apo-8′ carotenal consist of almost only the simple adsorbates and ester-like linkage form. Taking the triplet absorption spectrum of the model compound as that for the ester-like linkage surface species, the relative compositions of the simple adsorbed forms can be determined. The results together with the compositions estimated at other excitation wavelengths are listed in Table 4. Averaging the results at three different excitation wavelengths, the average compositions of the surface species are given as follows: simple adsorbates, 3%; ester-like linkage form, 63%; and bridging plus chelating form, 34%. Therefore, we conclude that at pH 3, carboxylic group anchoring on the colloidal TiO_2 surface in hexanol solution is mainly through the ester-like linkage binding, while the bridging and chelating forms also constitute a substantial portion of the surface binding forms. This result seems contradictory to the believed picture that the dye adsorbate−oxide binding is through chelation of surface titanium ions, however these authors referred to dyes with anchoring groups other than a single carboxylic group, where the two chelating oxygen atoms are not bonded to the same carbon atom. In this way the steric tension for chelation could be small,[51−53] and the surface coordination species can gain additional stability energy by the chelation effect. Though ATRA is quite different from the ruthenium complex dye in the structure, it provides general information regarding the binding forms of carboxylic groups at the TiO_2 surface. Experiments on TiO_2 film are going to be conducted; the results would be more directly related to the TiO_2 photoelectrode in solar cells.

TABLE 3: Time Constants from Monoexponential Fitting of the Observed Kinetics at Selected Wavelengths for Three Different Excitation Wavelengths

excitation λ(nm)	time constant (μs) at the selected λ (nm)			
	420	440	455	480
355	59.9 ± 8.0	49.2 ± 2.0	49.3 ± 3.0	51.9 ± 4.0
420	44.5 ± 8.0	45.8 ± 4.5	55.6 ± 5.6	62.5 ± 10.0
435	52.5 ± 10.1	49.5 ± 4.3	50.3 ± 6.7	54.0 ± 9.5

TABLE 4: Composition of ATRA/TiO_2 Surface Binding Forms in Hexanol Evaluated at Three Different Excitation Wavelengths

excitation λ(nm)	physical/hydrogen-bonding (%)	ester-like linkage (%)	bridging/chelating (%)
355	11	58	31
420	0	67	33
435	0	61	39

The nature of the binding forms can be affected by a number of factors such as the solvents, pH of the medium, co-anchoring groups in addition to the single carboxylic group, and the surface properties of the TiO_2 nanoparticles, as discussed above. It has been shown that in the aqueous solution the monocarboxylic acids are often weakly adsorbed to the TiO_2 surface as revealed by an in situ infrared spectroscopic study.[54] The result of our recent study by use of the same molecular probe technique also confirms that in the TiO_2 aqueous solution at pH 2, the simple adsorption form of carboxylate anion becomes more pronounced.[55] Considering the dye-sensitized mesoporous TiO_2

crystalline liquid solar cell employs anhydrous media,[7,8] and furthermore it has been shown that the dicarboxylic acids show more pronounced surface binding via ester-like linkage,[56] combining our present results it is concluded that the ester-like linkage can be the major surface binding form in the Grätzel cell.

Conclusions

We have shown that ATRA is an interface-sensitive molecular probe which can be used to detect the surface binding between a carboxylic group and the TiO_2 surface. The principle underlying this technique is the photoinduced interfacial back electron transfer to the triplet state, which renders the ATRA molecule the capability of reporting its different surface binding forms. By characterization of the triplet absorption spectra of ATRA in different forms, a part of the surface binding forms can be determined. At pH 3, the main surface species on a TiO_2 nanoparticle surface in hexanol solution is the ester-like linkage form, which constitutes about 63% of the total surface binding molecules. The chelating and bridge forms are difficult to identify individually, but together both of these surface species constitute 34% of the total. The simple adsorption forms including hydrogen bonding and anion forms contribute the remaining 3%. Our results provide quantitative evidence that the dye adsorbed onto a TiO_2 surface through a carboxylic group is mainly via ester-like linkage in hexanol at pH 3. By using the empirical relations, the ground state and the triplet energy levels for the three different surface species, i.e., ester-like linkage, bridge, and chelating forms have been evaluated. The evaluated ground-state absorption can be found for their corresponding counterparts in the experimental observations.

Acknowledgment. We thank Prof. J. P. Zhang and Dr. J. Feng in the Institute of Chemistry, Chinese Academy of Sciences, for their kind help in the confirmation of ATRA/TiO_2 transient absorption spectra by use of an OMA-assisted submicrosecond flash photolysis apparatus. Prof. Yasushi Koyama is acknowledged for his kind suggestions and comments. This work was supported by the Chinese National Key Basic Research and Development Plan under Grant G1998010102.

References and Notes

(1) Will, G.; Boschloo, G.; Hoyle, R.; Rao, S. N.; Fitzmaurice, D. *J. Phys. Chem. B* **1998**, *102*, 10272−10278.
(2) Colvin, V. L.; Schlamp, M. C.; Alivisatos, A. P. *Nature* **1994**, *370*, 354−357.
(3) Linsebigler, A. L.; Lu, G.; Yates, J. T., Jr. *Chem. Rev.* **1995**, *95*, 735−758.
(4) Hagfeldt, A.; Grätzel, M. *Chem. Rev.* **1995**, *95*, 49−68.
(5) Moser, J. E.; Bonnote, P.; Grätzel, M. *Coord. Chem. Rev.* **1998**, *171*, 245−250.
(6) O'Regan, B.; Grätzel, M. *Nature* **1991**, *353*, 737−739.
(7) Kay, A.; Grätzel, M. *Sol. Energy Mater. Sol. Cells* **1996**, *44*, 99−117.
(8) Nazeeruddin, M. K.; Kay, A.; Rodicio, I.; Humphry-Baker, E.; Muller, P. L.; Vlachopoulos, N.; Grätzel, M. *J. Am. Chem. Soc.* **1993**, *115*, 6382−6390.
(9) Shklover, V.; Ovchinnikov, Y. E.; Braginsky, L. S.; Zakeeruddin, S. M.; Grätzel, M. *Chem. Mater.* **1998**, *10*, 2533−2541.
(10) Braginsky, L.; Schklover, V. J. *Solid State Commun.* **1998**, *105*, 701.
(11) Ellingson, R. J.; Asbury, J. B.; Ferrere, S.; Ghosh, H. N.; Sprague, J. R., Lian, T.; Nozik, A. J. *J. Phys. Chem. B* **1998**, *102*, 6455−6458.
(12) Asbury, J. B.; Hao, E.; Wang, Y.; Ghosh, H. N.; Lian, T. *J. Phys. Chem. B* **2001**, *105*, 4545−4557.
(13) Benkö, G.; Kallioinen, J.; Korppi-Tommola, J. E. I.; Yartsev, A. P.; Sundström, V. *J. Am. Chem. Soc.* **2002**, *124*, 489−493.
(14) Meyer, T. J.; Meyer, G. J.; Pfennig, B. W.; Schoonover, J. R.; Timpson, C. J.; Wall, J. F.; Kobusch, C.; Chen, X.; Peck, B. M.; Wall, C. G.; Ou, W.; Erickson, B. W.; Bignozzi, C. A. *Inorg. Chem.* **1994**, *33*, 3952−3964.
(15) Murakoshi, K.; Kano, G.; Wada, Y.; Yanagida, S.; Miyazaki, H.; Matsumoto, M.; Murasawa, S. *J. Electroanal. Chem.* **1995**, *396*, 27−34.
(16) Grätzel, M. *Proc. Indian Acad. Sci. (Chem. Sci.)* **1995**, *107*, 607−619.
(17) Hugot-Le Goff, A.; Falaras, P. *J. Electrochem.* **1995**, *142*, L38−L41.
(18) Finnie, K. S.; Bartlett, J. R.; Woolfrey, J. L. *Langmuir* **1998**, *14*, 2744.
(19) Shklover, V.; Ovchinnikov, Y. E.; Braginsky, L. S.; Zakeeruddin, S. M.; Grätzel, M. *Chem. Mater.* **1998**, *10*, 2533−2541.
(20) Anderson, S.; Constable, E. C.; Dare-Edwards, M. P.; Goodenough, J. B.; Hamnett, A.; Seddon, K. R.; Wright, R. D. *Nature* **1979**, *280*, 571−573.
(21) Dare-Edwards, M. P.; Goodenough, J, B.; Andrew, A.; Seddon, K. R.; Wright, R. D. *Faraday Discuss.* **1981**, *70*, 285.
(22) Miyamae, T.; Nozoye, H. *J. Photochem. Photobiol. A: Chem.* **2001**, *145*, 93−99.
(23) Cherian, S.; Wamser, C. C. *J. Phys. Chem.* . **2000**, *104*, 3624−3629.
(24) Sasahara, A.; Uetsuka, H.; Onishi, H. *J. Phys. Chem. B* **2001**, *105*, 1−4.
(25) Duffy, N. W.; Dobson, K. D.; Gordon, K. C.; Robinson, B. H.; McQuillan, A. J. *Chem. Phys. Lett.* **1997**, *266*, 451−455.
(26) Umapathy, S.; Carmer, A. M.; Parker, A. W.; Hester, R. E. *J. Phys. Chem.* **1990**, *94*, 8880−8885.
(27) Couzis, A.; Gulari, E. *Langmuir* **1993**, *9*, 3414
(28) Sperline, R. P.; Freiser, H. *Langmuir* **1990**, *6*, 344.
(29) Vinodgopal, K.; Hua, X.; Dahlgren, R. L.; Lappin, A. G.; Patterson, L. K.; Kamat, P. V. *J. Phys. Chem.* **1995**, *99*, 10883−10889.
(30) O'Regan, B.; Grätzel, M.; Fitzmaurice, D. *J. Phys. Chem.* **1991**, *95*, 10525−10528.
(31) Tulock, J. J.; Blanchard, G. J. *J. Phys. Chem. B* **1998**, *102*, 7148−7155.
(32) Rakiewicz, E. F.; Peters, A. W.; Wormsbecher, R. F.; Sutovich, K. J.; Mueller, K. T. *J. Phys. Chem. B* **1998**, *102*, 2890−2896.
(33) Vasilescu, M.; Caragheorghepol, A.; Caldararu, H.; Bandula, R.; Lemmetyinen, H.; Joela, H. *J. Phys. Chem. B* **1998**, *102*, 7740−7751.
(34) Weng, Y. X.; Xiao, H.; Chan, K. C.; Che, C. M. *J. Phys. Chem. B* **2000**, *104*, 7713−7724.
(35) Weng, Y. X.; Xu, J. Z.; Pan, J.; Lin, K. L.; Wang, L.; Yang, G. Z. *Acta Bot. Sin.* **2000**, *42*, 1215−1219.
(36) Weng, Y. X.; Li, L.; Liu, Y.; Wang, L.; Yang, G. Z.; Sheng, J. Q. *Chem. Phys. Lett.* **2002**, *355*, 294−300.
(37) Porter, G.; Windsor, M. W. *J. Chem. Phys.* **1953**, *21*, 2088.
(38) Kliger, D. S.; Albrecht, A. C. *J. Chem. Phys.* **1970**, *53*, 4059−4065.
(39) Porter, G.; Windsor, M. W. *Proc. Royal Soc. A* **1958**, *245*, 239−258.
(40) Lo, K. K. N.; Land, E. J.; Truscott, T. G. *Photochem. Photobiol.* **1982**, *36*, 139−145.
(41) Bobrowski, K.; Das, P. K. *J. Phys. Chem.* **1985**, *89*, 5079−5080.
(42) Bensasson, R.; Land, E. J.; Truscon, T. G. *Photochem. Photobiol.* **1973**, *17*, 53.
(43) Pan, J.; Benkö, G.; Xu, Y.; Pascher, T.; Sun, L.; Sundström, V.; Polívka, T. *J. Am. Chem. Soc.* **2002**, *124*, 13949−13957.
(44) Zhang, L.; Weng, Y. X.; et al., to be submitted for publication.
(45) Marcus, R. A.; Sutin, N. *Biochim. Biophys. Acta* **1985**, *811*, 265.
(46) Becker, R. S.; Bensasson, R. V.; Lafferty, J.; Truscott, T. G., Land, E. J. *J. Chem. Soc., Faraday Trans.* **1978**, *274*, 2246−2255.
(47) Sanjinés, R.; Tang, H.; Berger, H.; Gozzo, F.; Margaritondo, G.; Lévy, F. *J. Appl. Phys.* **1994**, *75*, 2945−2951.
(48) Göpel, W.; Anderson, J. A.; Frankel, D.; Jaehnig, M.; Phillips, K.; Schäfer, J. A.; Rocker, G. *Surface Sci.* **1984**, *139*, 333−346.
(49) Truscott, T. G.; Land, E. J.; Sykes, A. *Photochem. Photobiol.* **1973**, *17*, 43−51.
(50) Turro, N. J. *Modern Molecular Photochemistry*; University Science Book: Sausalito, CA, 1991.
(51) Moser, J.; Punchihewa, S.; Infelta, P. P.; Grätzel, M. *Langmuir* **1991**, *7*, 3012−3018.
(52) Frei, H.; Fitzmaurice, D. J.; Grätzel, M. *Langmuir* **1990**, *6*, 198−206.
(53) Redmond, G.; Fitzmaurice, D.; Grätzel, M. *J. Phys. Chem.* **1993**, *97*, 6951−6954.
(54) Dobson, K. D.; McQuillan, A. J. *Spectrochim. Acta A* **1999**, *55*, 1395−1405.
(55) Zhang, Q. L.; Du, L. C.; Weng, Y. X., unpublished results.
(56) Dobson, K. D.; McQuillan, A. J. *Spectrochim. Acta A* **2000**, *56*, 557−565.